

# Tropical Atmosphere-Ocean Interactions in a Conceptual Framework

Malte F. Jansen\*, Dietmar Dommenges† and Noel Keenlyside  
Leibniz Institut für Marine Sciences, Kiel, Germany

Journal of Climate, accepted, August 7, 2008

---

\*Current affiliation: Program in Atmospheres, Oceans and Climate, Massachusetts Institute of Technology, Cambridge, Massachusetts, USA

†*Corresponding author address:* Dietmar Dommenges, Leibniz Institut für Meereswissenschaften, Düsterbrooker Weg 20, D-24105 Kiel, Germany  
E-mail: ddommenget@ifm-geomar.de

## Abstract

Statistical analysis of observations (including atmospheric reanalysis and forced ocean model simulations) is used to address two questions: First, does an analogous mechanism to that of the El Niño Southern Oscillation (ENSO) exist in the equatorial Atlantic or Indian Ocean? Second, does the intrinsic variability in these basins matter for ENSO predictability? These questions are addressed by assessing the existence and strength of the Bjerknes and delayed-negative feedbacks in each tropical basin, and by fitting conceptual recharge-oscillator models, with and without interactions among the basins.

In the equatorial Atlantic the Bjerknes and delayed-negative feedbacks exist, although weaker than in the Pacific. Equatorial Atlantic variability is well described by the recharge oscillator model, with an oscillatory mixed ocean dynamics-sea surface temperature (SST) mode present in boreal spring and summer. The dynamics of the tropical Indian Ocean, however, appear to be quite different: No recharge-discharge mechanism is found. Although, some positive Bjerknes feedbacks from July to September are found, the role of heat content seems secondary.

Results also show that Indian Ocean interaction with ENSO tends to damp the ENSO oscillation and is responsible for a frequency shift to shorter periods. However, the retrospective forecast skill of the conceptual model is hardly improved by explicitly including Indian Ocean SST. The interaction between ENSO and the equatorial Atlantic variability is weaker. However, a feedback from the Atlantic on ENSO appears to exist, which slightly improves the retrospective forecast skill of the conceptual model.

# 1. Introduction

The atmosphere-ocean interactions responsible for ENSO are well understood and can be described by simple conceptual models, such as the delayed action oscillator (Suarez and Schopf, 1988; Battisti and Hirst, 1989) and the recharge oscillator model (Jin, 1997). There are also indications, that a similar coupled mode exists in the Atlantic Ocean (e.g., Zebiak, 1993; Latif and Grötzner, 2000; Keenlyside and Latif, 2007). Keenlyside and Latif (2007) show that all elements of the Bjerknes feedback, which allows for the growth of an initial perturbation via Atmosphere-Ocean interaction, are active in the equatorial Atlantic. However, they do not analyze the existence of a delayed negative feedback, which is necessary for the oscillatory behavior of ENSO in the Pacific. In the recharge oscillator picture, this negative feedback acts via the discharge/recharge of equatorial averaged heat content.

Webster et al. (1999) and Saji et al. (1999) first suggested that a zonal dipole mode in the Indian Ocean is a reflection of atmosphere-ocean interaction intrinsic to the Indian Ocean. Whether or not this can be understood as an oscillatory mode of internal Atmosphere-Ocean dynamics in the Indian Ocean is currently still under discussion (e.g., Baquero-Bernal et al., 2002; Dommenges and Latif, 2002; Behera et al., 2003; Dommenges and Latif, 2003; Behera et al., 2006). Several recent publications argue or indicate that elements of a Bjerknes type of feedbacks are active in the Indian Ocean supporting the Indian Ocean dipole mode (e.g., Gualdi et al., 2003; Fischer et al., 2005; Behera et al., 2006; Chang et al., 2006b; Song et al., 2007).

While it is known that the Indian Ocean responds strongly to ENSO (e.g., Venzke et al., 2000), recent studies also suggest a feedback of the Indian Ocean SST on ENSO (Yu et al., 2002; Wu and Kirtman, 2004; Yu, 2005; Annamalai et al., 1995; Kug and Kang, 2006; Dommenges et al., 2006; Yeh et al., 2007). Analyzing observational data, Kug and Kang (2006) suggest a negative feedback from the tropical Indian Ocean on ENSO. CGCM experiments on the influence of the Indian Ocean on the ENSO cycle come to conflicting results: Yu et al. (2002) find that ENSO variability is decreased and the frequency is slightly increased, if the Indian Ocean is decoupled from the system. Wu and Kirtman (2004) agree that ENSO variability is decreased, but find that the frequency is also decreased if the Indian Ocean is decoupled. Dommenges et al. (2006) agree with the latter that the ENSO frequency is decreased, but find increased ENSO variability if the Indian Ocean is decoupled from the system.

It is generally agreed that ENSO influences the North (e.g., Enfield and Mayer, 1997) and South Tropical Atlantic. ENSO's influence on the equatorial Atlantic is, however, less clear (Zebiak, 1993; Enfield and Mayer, 1997; Saravanan and Chang, 2000; Ruiz-Barradas et al., 2000; Latif and Grötzner, 2000; Huang, 2004). Recently it has been suggested that this is due to ENSO's competing dynamical and thermodynamical influences there (Chang et al., 2006a). On the otherhand, the strongest correlation between Niño3 SST anomalies (SSTA) and eastern equatorial Atlantic SSTA is negative and occurs when the Atlantic leads the Pacific by about 6 month (Keenlyside and Latif, 2007). This may imply that there is a feedback from the Atlantic on ENSO, which in turn may have implications for ENSO prediction. An indication for such a feedback was also found in Wang (2006).

This study analyses if the recharge mechanism, which is necessary for the oscillatory behavior of ENSO (Zebiak and Cane, 1987; Jin, 1997), exists in the equatorial Atlantic and Indian Oceans and whether it is strong enough to allow oscillatory behavior. This is done in two ways. First, the elements of the Bjerknes feedbacks and the delayed negative feedback in the three different oceans are compared. This and all analysis are computed using observed SST, NCEP/NCAR surface stress, and 20°C-isotherm depth anomalies from a forced ocean model

simulation. Second, the conceptual recharge oscillator model (Burgers et al., 2005) is fit to Atlantic and Indian Ocean data. The parameters found are discussed in terms of whether or not they support the recharge mechanism or whether they point to a different mechanism. The relevance of the model is assessed by how well it reproduces observed statistics and by its performance in retrospective forecasts.

Furthermore, simple models are proposed as hypotheses for the interaction of the tropical Atlantic and Indian Oceans with ENSO. Model parameters are fitted to observational data and the implications of the resulting parameters for the impact of the Indian and Atlantic Ocean on the ENSO cycle are analyzed.

This paper is organized as follows. The data and methods are described in section 2. The elements of the Bjerknes and delayed negative feedback in the three tropical oceans are compared in section 3. The recharge oscillator model fits to Atlantic and Indian Ocean observations are described in section 4. A simple statistical model analysis for the interactions between ENSO and the Indian and Atlantic Oceans is presented in section 5. Section 6 concludes with a summary and discussion.

## 2. Data and Methods

Observational SST data are taken from the HadISST 1.1 data set (Rayner et al., 2003). Zonal wind stress data are from the NCEP/NCAR reanalysis (Kalnay et al., 1996). As subsurface ocean observations are scarce outside of the equatorial Pacific and prior to the mid-1980's,  $20^\circ$  isotherm depth are from an NCEP/NCAR reanalysis forced simulation from 1948 to 2001 of the MPI-OM ocean general circulation model (OGCM) (Marsland et al., 2003); Standard bulk formulas for the calculation of heat fluxes and a weak relaxation of surface salinity to the Levitus et al. (1994) climatology are used. Data from the simulation were used in a previous study of equatorial Atlantic variability (Keenlyside and Latif, 2007), where results were carefully checked against those obtained from various observations, including XBT and Topex/Poseidon SLA, for the Pacific and Atlantic oceans. Furthermore, we repeated our analysis with SODA (Carton et al., 2000) and found very similar results.

The various area average indices and linear combinations of these that we use (table 1) generally conform with those in the literature. The Indian Ocean dipole-mode index, however, is used with the reversed sign (i.e., the eastern pole minus western pole) and it is denoted (-)DMI. This definition facilitates easier comparison with the analysis of feedbacks in the Pacific and Atlantic. Following Meinen and McPhaden (2000), equatorial warm water volume (WWV) of an ocean basin is defined as the volume of water warmer than  $20^\circ\text{C}$  between  $5^\circ\text{S}$ - $5^\circ\text{N}$  in that basin. In all subsequent analysis data are linearly detrended and the seasonal cycle is removed. The significance of the results is estimated using the standard 2-sided student-t test.

The parameters of the simple models used in the subsequent analysis are estimated by fits to monthly mean indices from the observational and GCM data described above. The fits minimize the rms error of the models for 1-month forecasts of the index time series. Confidence levels for the parameter values are estimated using a multi-linear regression. For the seasonal dependent parameter fits, a 3 month moving data block is used for each monthly parameter set (i.e. the parameters for the March-April transition, for example, are fitted using all data from February, March and April for the predictors and all data from March, April and May for the response variables).

### 3. The positive Bjerknes and delayed negative feedbacks

In this section, the existence of positive Bjerknes and delayed negative feedbacks in the equatorial Atlantic and Indian Ocean are investigated, and contrasted against those of the Pacific. A more detailed analysis of the positive feedback in the Atlantic is given by Keenlyside and Latif (2007).

Conceptually, the positive Bjerknes feedback consists of three elements: (1) forcing of surface winds in the west by SSTA in the east, (2) forcing of heat content anomalies in the east by winds to the west, and (3) the forcing of SSTA in the east by heat content anomalies there. The existence and strength of the first element of the positive Bjerknes feedback is assessed by regressing SST indices onto surface zonal wind stress (Fig. 1a). In the Pacific, a  $1^{\circ}\text{C}$  SSTA in the east is associated with westerly zonal wind stress of up to  $1.1 \cdot 10^{-2} Pa$  (45% explained variance) over the central Pacific. In the Atlantic there is similar but weaker picture ( $0.8 \cdot 10^{-2} Pa/1^{\circ}\text{C}$  and 25% exp. variance).

In the Indian Ocean an anomalous east-west SST difference of  $1^{\circ}\text{C}$  is associated with zonal wind stress anomalies of up to  $2.0 \times 10^{-2} Pa$  (25% exp. variance). Regression patterns are similar in structure when individual poles of the (-)DMI are considered separately, but explained variances are lower (5%; not shown). Regression strength remains similar for the western pole, but for the eastern pole it is much weaker and of similar strength to that of the Pacific. Note that the regression pattern is of one sign over the eastern box in all three cases; consistent with a local response of winds to SST in the eastern box.

The second element of the positive Bjerknes feedback is estimated by regressing indices of surface zonal wind stress anomalies onto anomalous  $20^{\circ}\text{C}$ -isotherm depth (Fig. 1b). Central Pacific zonal wind stress anomalies are associated with a deeper thermocline over eastern Pacific, and shallow thermocline in the west, particularly off the equator. The largest values are found in the east, where a  $1 \times 10^{-2} Pa$  anomaly is associated with thermocline depth anomalies of 20m (45% exp. variance). Western Atlantic zonal wind stress anomalies produce a similar, although weaker relationship ( $5-8m[10^{-2} Pa]^{-1}$ ) and explaining less variance (25%). In the Indian Ocean the relationship in the east is similar to that in the Atlantic.

The third element of the positive Bjerknes feedback is estimated by regressing subsurface  $20^{\circ}\text{C}$ -isotherm depth anomalies onto SSTA (Fig. 1c). In the eastern Pacific, the relationship is strongest (2-3K per 100m) and explains the most variance (45%). A similar relationship is found in the Atlantic, but explained variance is around half. In the Indian Ocean, almost no relationship exists, except off the coast of Java-Sumatra and in the central south tropical region, as previously identified (Xie et al., 2002).

Analysis of the cross correlation functions can provide further insight on the feedbacks. The cross-correlation between Niño3 SSTA and Niño4 zonal wind stress anomalies reflects the accepted existence of a positive Bjerknes feedback: a near symmetric curve, with wind stress anomalies leading the SST by one-to-two months (Fig. 2a). Positive correlations at positive lag indicate SST forcing of the atmosphere, and vice versa for negative lags. The one-to-two month lead of the atmosphere is consistent with a non-local response. The corresponding cross-correlation function for the Atlantic has a similar structure to that of the Pacific (Fig. 2a), however, correlations are weaker and the positive peak narrower.

The cross-correlation function for the Indian Ocean (Fig. 2a) is weaker than that of the Atlantic and wind anomalies tend to lag SSTA instead of leading. The cross-correlation functions recomputed separately for the eastern and western poles of the (-)DMI SSTA index (Fig. 2a) reveal three points: First, correlations are much weaker and hardly significant. Second, east-

ern pole SSTA lead central equatorial Indian Ocean zonal wind stress anomalies. This relation may result from local feedbacks, such as the wind-evaporation-SST and coastal upwelling feedbacks that are active during boreal summer and autumn (Chang et al., 2006b). There is, however, little evidence from the cross-correlation function that these (remote) wind anomalies in turn feedback on the SSTA. Third, central Indian Ocean wind stress lead western pole SSTA. These SSTA may, for instance result from anomalous surface Ekman currents caused by the wind anomalies. The cross-correlation function suggests they do not feedback on the wind-anomlies. Thus for the Indian Ocean, the cross-correlation functions provide little evidence for a large-scale Bjerknes like positive feedback involving the SSTA and zonal wind stress indices considered here, and considering all seasons. This doesn't preclude the existence of other types of feedbacks.

The cross-correlation function between Niño3 SSTA and 20°C-isotherm depth is consistent with subsurface temperature anomalies forcing SSTA (Fig. 2b): correlations are maximum when 20°C-isotherm depth anomalies lead SSTA by one month and remain positive out to one year. A similar, albeit weaker relationship exists in the Atlantic (Fig. 2b). The picture for the Indian Ocean is almost the reverse of the other basins: (-)DMI SSTA precede 20°C-isotherm depth anomalies, with maximum correlation when SSTA lead by two months, and positive correlations extend longer when SSTA lead rather than lag (Fig. 2b). The cross-correlation function computed using only the eastern pole of the (-)DMI (Fig. 2b) shows little evidence that subsurface temperature anomalies impact SST, but instead suggest the converse (probably via the atmospheric response to SSTA). Correlations for the western pole (Fig. 2b), although hardly significant, are consistent with subsurface temperature anomalies forcing SSTA.

The seasonality of variability may result from seasonality in the three elements of the Bjerknes feedback, as Keenlyside and Latif (2007) showed for the Atlantic. To investigate if this may also be the case for Indian Ocean variability, the above cross-correlation analysis was repeated for each calendar month (not shown). The cross-correlations involving the (-)DMI eastern pole are the most interesting. They are strongest in boreal summer and autumn, exceeding 0.6, and stronger than correlations computed for all months (Fig. 2). The lead-lag relationships, however, remain similar. An exception is that July to September (-)DMI (and eastern pole) SSTA tend to follow central equatorial Indian Ocean zonal wind anomalies by about one month. This may be indicative of a positive Bjerknes type feedback. However, the maximum correlation between SST and subsurface temperature anomalies (at the eastern pole) in these seasons is with SST leading by at least a month. Thus, while heat content variations likely contribute to such a feedback (given the high correlation in these seasons), they do not play a dominant role. The cross-correlation analysis was also performed considering only (-)DMI years with ENSO years excluded (definitions following Meyers et al. (2007)). Although correlations are (not surprisingly) stronger, relationships among SST, zonal wind, and heat content indices remain similar. Thus the above findings are robust to the event like nature of (-)DMI variability.

The oscillatory nature of ENSO arises from a delayed negative feedback produced by the discharge-recharge of heat content between the tropics and sub-tropics. As already shown by Meinen and McPhaden (2000), in the Pacific WWV leads equatorial SSTA, with maximum positive correlations for lead times between three and six months (Fig. 3a). Consistent with the ENSO spring predictability barrier, weakest correlations occur for spring time SSTA. Strong negative correlations occur when SSTA lead WWV anomalies by between six to twelve months. (Correlations shown are weaker than those of Meinen and McPhaden (2000), as we use an ocean model simulation and consider a different period.)

In the Atlantic the picture is broadly consistent with that of the Pacific: generally positive

(negative) correlations when WWV anomalies lead (lag) SSTA (Fig. 3b). However, there are three important differences: First, correlations are significantly weaker, indicating a lesser importance of this mechanism in the Atlantic. Second, a delayed negative feedback is primarily seen only from April to August. Third, for boreal summer, the seasons of strongest SST variability, there appears to be a predictability barrier. Despite these differences, a delayed negative feedback appears present in the Atlantic.

The picture in the Indian Ocean is almost the converse of the Pacific: positive correlations occur primarily when SSTA lead WWV anomalies, and the largest negative correlation is when WWV anomalies lead boreal winter SSTA (Fig. 3c). The correlations are also the weakest of all three basins. It may be speculated that the east-west tilt in thermocline depth may be a more appropriate index than WWV. However, similar results are found when the analysis is repeated using instead the (-)DMI 20°C-isotherm depth. Thus, the discharge-recharge of equatorial heat content variations in the Indian Ocean has little influence on SST.

In summary, linear regression analysis of positive and negative feedbacks in the three tropical oceans indicates the existence of similar dynamics in the Pacific and Atlantic, although in the latter the mechanism explains less variance. In the Indian Ocean we find some evidence for a positive feedback during July to September. Though heat content variations do not seem to play a dominant role in forcing SSTA. Note the stationarity of the above results was checked by recomputing the analysis for periods before and after the 1970's climate shift. While relationship generally strengthen following the climate shift, particularly in the Indian Ocean, the main findings above are unchanged.

## 4. The Recharge Oscillator for Atlantic and Indian Ocean

Following Burgers et al. (2005), the recharge oscillator model for ENSO can be written as

$$\frac{d}{dt} \begin{pmatrix} T_E \\ h \end{pmatrix} = \begin{pmatrix} a_{11} & a_{12} \\ a_{21} & a_{22} \end{pmatrix} \begin{pmatrix} T_E \\ h \end{pmatrix} \quad (1)$$

where  $a_{ij}$  are model parameters,  $T_E$  denotes eastern Pacific SSTA and  $h$  denotes thermocline depth averaged over the whole equatorial Pacific basin, in the original ENSO model. In the analogous application of the model to the Atlantic/Indian Ocean,  $T_E$  denotes the Atlantic/Indian Ocean SSTA and  $h$  denotes thermocline depth averaged over the equatorial Atlantic/Indian Ocean basin. Note, that the models based on these equation only represent a recharge mechanism, if the eigenvalues/parameters suggest the right coupling between  $T_E$  and  $h$ . The model may reduce to a simple linear damped uncoupled system if no significant coupling exist.

### a. Atlantic Ocean

The model is fit for the period 1951-2001 using Atl3 SSTA for  $T_E$  and equatorial Atlantic WWV for  $h$ . Parameters are fitted for each calendar month as described in section 2.

The seasonal cycle of the eigenvalues of equation (1), for the Atlantic data (Fig. 4a) shows that an oscillatory mode exists from boreal spring till early fall, that can be identified as a mixed SST-thermocline depth mode, by looking at the corresponding eigenvectors (not shown). There are two peaks in growth rate, one in April and another in October. The first may be related to the summer time Atlantic Niño and the latter to the Atlantic Niño II identified by Okumura and Xie (2006). The system is over-damped with two decaying eigenmodes in late fall and winter. For the Pacific, in agreement with Burgers et al. (2005), parameters corresponding

to oscillatory eigenmodes are found nearly throughout the whole year (Fig.4b). While in the Pacific growth rates are around zero in late summer/early fall, only decaying modes are found in the Atlantic throughout the whole year. The damping is smallest in early boreal spring, which is in agreement with the observed maximum in the variance of eastern Atlantic SSTA in early summer.

To assess the goodness of fit to observed statistical parameters (e.g., spectrum or cross-correlation), equation (1) is integrated forward in time. Stochastic forcing on SST ( $\xi_T$ ) and thermocline depth ( $\xi_h$ ) is used to excite variability, as proposed by Jin (1997). Physically, they represent wind and heat flux forcing due to short time-scale uncoupled atmospheric variability and are approximated by white noise. The variances of the noise forcing are chosen to reproduce observed variances of SSTA and thermocline depth, and satisfy  $\sigma_{\xi_h} = 0.6 \cdot \sigma_{\xi_T}$ . For simplicity they are assumed to be independent. Even though the forcing parameters are constant throughout the year, the model produces a seasonal cycle in the variance of eastern Atlantic SST that is in good agreement with observations (not shown).

The seasonally resolved cross correlation between Atl3 SSTA and Atlantic WWV from the simple model integration (Fig. 5) agrees well with the observed cross correlation (Fig.3b), indicating that the elementary surface-subsurface interaction is well described by the simple model approach.

Figure 6a shows the power spectral density of SST ( $\Gamma_{SST}$ ) resulting from the model integration, compared to  $\Gamma_{SST}$  from 1870-2003 observational Atl3 data. The model spectrum as well as the observed spectrum are hardly distinguishable from that of a red noise process. Figure 6b shows that, compared to a fitted AR1 process, variance in the recharge oscillator model is somewhat increased on interannual time scales, with a peak frequency around 4 years.

The model is integrated in forecast mode using observed SST and thermocline depth data for initialization. Forecast runs are started from each month and integrated for one year. For both cross validated time periods, forecast skill above persistence is found (Fig. 7a). It should be added that even better forecast skill may be expected if real observational thermocline depth data would be available instead of the NCEP forced OGCM data that is used here. (As is the case for the Pacific.)

To test the importance of internal atmosphere-ocean dynamics in the equatorial Atlantic versus the remote forcing of ENSO, an AR1 model with an additional forcing from ENSO is fit to observational SST data for the same time period. The model can be written as:

$$T_E(t + 1 \text{ month}) = \alpha \cdot T_E(t) + c_{AP} \cdot T_P(t) \quad (2)$$

where  $T_E$  is Atl3 SSTA and  $T_P$  is Niño3 SSTA. Parameters,  $\alpha$  and  $c_{AP}$  are fit for each calendar month, as for the recharge oscillator model. The forecast skill of this model (fig. 7b) is hardly better than persistence, indicating that internal coupled atmosphere-ocean dynamics are important in the eastern equatorial Atlantic, and that the variability there cannot be viewed simply as a damped response to remote ENSO forcing.<sup>1</sup>

### *b. Indian Ocean*

Parameters of the recharge oscillator model are fit to Indian Ocean observations, as done for the Atlantic in the previous section. The reversed Indian Ocean Dipole mode ((-)DMI) is used for  $T_E$  in equation (1), instead of a single area in the eastern basin as for the Pacific and

---

<sup>1</sup>Niño3 SSTA is not predicted in the forecast integrations of (2), but taken from observations, so this model contains artificial skill due to the knowledge of Niño3 SSTA.

Atlantic Oceans. Equatorial Indian Ocean WWV is taken for  $h$ . Note, that the qualitative results presented in the following change little, if only the eastern part of the dipole mode, or an index centered in the eastern equatorial Indian Ocean is chosen for  $T_E$ .

The seasonal cycle of the eigenvalues show, that no significant oscillatory mode exists (Fig. 8). Except for the June-July transition, two damped eigenmodes are found throughout the year. Looking at the corresponding eigenvectors (not shown), especially for boreal fall and winter, the amplitude of the stronger damped mode can be identified approximately with a pure SST mode. The weaker damped eigenvalue on the other hand belongs to a mode that is approximately a pure thermocline depth mode. Indeed, comparing the eigenvalues to the SST and thermocline depth damping parameters  $a_{11}$  and  $a_{22}$  (not shown), one finds that for the major part of the year the two damping time scales match the damping of SST and the thermocline depth anomalies. The weaker damping of SSTA in boreal summer is in agreement with the variability of the DMI peaking towards the end of summer. This reduced damping in boreal summer is not found for equatorial averaged Indian Ocean SSTA.

As for the Atlantic, the model is integrated forward in time to assess the goodness of fit to observed statistical parameters. The variances of the additional noise forcing are again fit to mimic the total variances of SSTA and thermocline depth. They are chosen to meet  $\sigma_{\xi_h} = 0.65 \cdot \sigma_{\xi_T}$ . The SST spectrum resulting from the model integration, as well as the observational spectrum (not shown), are not significantly different to a red noise spectrum. Figure 9 a) shows the seasonally resolved cross correlation between the (-)DMI and equatorial Indian Ocean WWV resulting from the model integration. As in the observed cross correlation (Fig. 3c) we find maximum correlation with late summer (-)DMI anomalies leading a WWV anomalies of the same sign in Fall. In the recharge oscillator picture for ENSO, the oscillation is caused by shallowing (deepening) of the averaged thermocline via wind stress changes induced by warm(cold) eastern ocean SSTA. This would correspond to negative correlations with (-)DMI anomalies leading WWV anomalies. The recharge mechanism can therefore not be found in the Indian Ocean. The eigenvalues and parameters of the model fitted rather suggest a mostly uncoupled linear damped system.

Forecast runs are started from each month and integrated for one year, as done for the Atlantic. Figure 10a shows that the recharge oscillator model does not have prediction skill above persistence for the DMI. To estimate to what extent the DMI is independent from ENSO, an AR1 model with an additional forcing from ENSO is fitted to observational DMI data, as done for the Atlantic in the previous section. Skill above persistence is found especially on long lead times (Fig. 10b). It should be mentioned that this is not a real forecast run, since Niño3 SST is not modeled, but prescribed from observations. The small, approximately constant forecast skill, on long time scales, is in agreement with the small, but significant correlation of the DMI with Niño3 SSTA. Figure 10c shows the results of the same model but for equatorial Indian Ocean SSTA (EqInd). It can be seen, that the averaged equatorial Indian Ocean SSTA is to a large extent determined by ENSO. The correlation skill of this model is higher, than the correlation between Niño3 and EqInd SSTA itself, which has a maximum of 0.61 with Niño3 SSTA leading EqInd SST by about three month, for 1950-2001 HadISST data.

## 5. Interactions with ENSO

A simple coupled model for the interactions of the Pacific with the Atlantic or Indian Ocean is presented in Dommenges et al. (2006). It consists of the simplest recharge oscillator model presented by Burgers et al. (2005) coupled to a linear damped model for the Atlantic or Indian

Ocean. It proposes a feedback from the Atlantic/Indian Ocean on Pacific SST. Kug and Kang (2006) propose a similar model but with a feedback on western equatorial thermocline depth. In the following, the model as used by Dommenges et al. (2006) is extended by a feedback of Indian/Atlantic Ocean SSTA on averaged Pacific thermocline depth. It can be written as

$$\begin{aligned}\frac{d}{dt}T_P &= \omega_0 h_P - 2\gamma_P T_P + c_{PI/PA} T_{I/A} \\ \frac{d}{dt}h_P &= -\omega_0 T_P + ch_{PI/PA} T_{I/A} \\ \frac{d}{dt}T_{I/A} &= -2\gamma_{I/A} T_{I/A} + c_{IP/AP} T_P\end{aligned}\quad (3)$$

where  $\omega_0$  is the coupling between  $T_P$  and  $h_P$ ,  $\gamma_{P/I/A}$  are the damping parameters,  $T_P$  is eastern Pacific (Niño3) SSTA,  $h_P$  denotes thermocline depth anomaly averaged over the equatorial Pacific and  $T_{I/A}$  is SSTA averaged over the equatorial Indian/Atlantic Ocean. The  $c_{IP/AP}$  term describes the coupling of the Indian/Atlantic Ocean on Pacific SSTA whereas  $c_{PI/PA}$  and  $ch_{PI/PA}$  represent the feedback of Indian/Atlantic Ocean SSTA on Pacific SST and thermocline depth, respectively.

Note, that some studies of the Indian Ocean interaction with ENSO may suggest a more complex interaction, not captured by this model, which may also be true for the Atlantic Ocean (e.g., Annamalai et al., 1995). However, in this first attempt of quantifying the feedback from observations, we have to note that the limited observational data may prevent us from using more complex models even though they may seem desirable.

#### a. Indian Ocean

The parameters of equation (3) are fitted to 1951-2001 Eqind and Niño3 SSTA. Note, that some studies suggest a regime shift in the Indian Ocean-ENSO relationship (e.g. Dominiak and Terray (2005)), but statistics are too short to evaluate this in the context of this work. The data and fitting methods are described in section 2. To reduce the number of degrees of freedom, a seasonal dependent parameter fit is not performed here. The resulting parameters and estimated 95% confidence intervals in units month<sup>-1</sup> are  $\gamma_P = 0.022 \pm 0.017$ ,  $\omega_P = 0.106 \pm 0.023$ ,  $\gamma_I = 0.135 \pm 0.017$ ,  $c_{IP} = 0.24 \pm 0.03$ ,  $c_{PI} = -0.053 \pm 0.035$  and  $ch_{PI} = -0.052 \pm 0.030$ . The strong coupling with Niño3 SSTA forcing Eqind SSTA,  $c_{IP}$ , is in agreement with many previous studies. Concerning the feedback of Indian Ocean SSTA onto ENSO we find that a warm(cold) Indian Ocean causes a cooling(warming) in the eastern Pacific and a shallowing(deepening) of the equatorial averaged thermocline in the Pacific, which is significant at the 95% confidence level. A possible explanation may be the response of the Walker circulation to warm(cold) Indian Ocean SST, which cause easterly(westerly) wind anomalies over the western equatorial Pacific and Indonesia. These wind anomalies could cause an upwelling(downwelling) in the western-central Pacific, which in turn causes a shallowing(deepening) of the averaged Pacific thermocline depth and a cooling(warming) in the eastern Pacific due to Kelvin wave propagation. However, this is speculation at this point and should be subject of further research.

To estimate the importance of the feedback from the Indian Ocean on ENSO and to explain the observed cross correlation, an alternative model is fit to observational data that is similar to (3) except that no feedback from the Indian Ocean on the Pacific is included. The fitted parameters are  $\gamma_P = 0.040 \pm 0.011$ ,  $\omega_P = 0.133 \pm 0.022$ ,  $\gamma_I = 0.136 \pm 0.022$  and  $c_{IP} = 0.25 \pm 0.04$ . Both models are integrated using the fitted parameters and an additional stochastic forcing on Indian Ocean SST ( $\xi_{T_I}$ ) and Pacific SST ( $\xi_{T_P}$ ) and thermocline depth ( $\xi_{h_P}$ ), to evaluate statistical parameters of this model against the observations. For simplicity,  $\xi_{T_I}$  is assumed to be independent of the Pacific noise forcing. However, some correlation between the Pacific forcing ( $\xi_{T_P}$  and  $\xi_{h_P}$ ) is necessary to mimic the total variance of observed Niño3 SST and

WWV. Since wind stress forcing acts on both, SST and WWV via different mechanisms, a correlation between the two forcing is physically reasonable, but the magnitude or even the sign of the correlation can not be easily estimated by physical reasoning. It is therefore fit to mimic the observations here. The noise forcing for the model with feedback are chosen to meet  $\sigma_{\xi_{h_P}} = 0.6 \cdot \sigma_{\xi_{T_P}}$ ,  $\sigma_{\xi_{T_I}} = 1.8 \cdot \sigma_{\xi_{T_P}}$  and the correlation between  $\xi_P$  and  $\xi_h$  is 0.5. For the model without feedback, they meet  $\sigma_{\xi_{h_P}} = 0.6 \cdot \sigma_{\xi_{T_P}}$ ,  $\sigma_{\xi_{T_I}} = 1.45 \cdot \sigma_{\xi_{T_P}}$  and the correlation between  $\xi_P$  and  $\xi_h$  is 0.2. It should be noted that since the equations are written for normalized variables, the stronger noise forcing of Indian Ocean SSTA compared to Niño3 SSTA denotes a higher signal to noise ratio in the Pacific, which is due to the fact that the major part of the Pacific SST variability is explained by the ENSO dynamics that are explicitly contained in the model.

Figure 11 shows the cross correlation of the two different models, compared to the observed cross correlation. The cross correlation of both coupled models fit well to observations, where the model with an Indian Ocean feedback on ENSO does resemble the observed cross correlation slightly better, particularly with regard to the phase.

The power spectral density of the coupled conceptual model given by equations (3) can be calculated analytically. Figure 12a shows the SST spectrum compared to the observed Niño3 SST spectrum, calculated from 1870-2003 HadISST data. The model spectrum fits well with observations. However, there seems to be a tendency to find a more pronounced peak and therefore a more regular behavior in the model.

Figure 12 b) shows the influence of the Indian Ocean feedback on ENSO. If the feedback is switched off (which means here that  $ch_{PI}$  and  $c_{PI}$  are set to zero) the peak frequency shifts to lower frequencies and the total variance is increased (the eigenfrequency shifts from 48.5 month<sup>-1</sup> to 60.5 month<sup>-1</sup> and the total variance is increased by 42%).

The forecast skill for Niño3 SSTA predictions of the coupled conceptual model used here, however, is hardly better than the forecast skill of the recharge oscillator model without a feedback from the Indian Ocean (fig. 13).

### *b. Atlantic Ocean*

Analogous to the previous section, the coupled model, described by equation (3), is now used to describe the interaction between the Atlantic Ocean and ENSO. The model parameters are fitted to 1951-2001 Atl3<sup>2</sup> and Niño3 SSTA data and equatorial Pacific WWV for h. The resulting parameters and estimated 95% confidence intervals in units month<sup>-1</sup> are  $\gamma_P = 0.040 \pm 0.015$ ,  $\omega_P = 0.131 \pm 0.0017$ ,  $\gamma_A = 0.073 \pm 0.015$ ,  $c_{AP} = 0.030 \pm 0.029$ ,  $c_{PA} = -0.025 \pm 0.029$  and  $ch_{PA} = -0.028 \pm 0.029$ .

Focusing on the parameters describing the interaction between the two oceans, one finds weaker interactions than between Indian Ocean and Pacific. Especially the coupling of Atl3 SSTA on Niño3 SSTA ( $c_{AP}$ ) is much weaker than the coupling of the Indian Ocean on ENSO. However, it is significantly different from zero, with an El Niño (La Niña) event causing a warming (cooling) in the Atl3 region. Concerning the Feedback of Atlantic Ocean SSTA on ENSO we find that a warm (cold) Atlantic causes a cooling (warming) in the Niño3 region and a shallowing (deepening) of the equatorial averaged thermocline in the Pacific, similar to the feedback of the Indian Ocean on ENSO. Both feedback parameters are different from zero at the 90% significance level, but do not pass the 95% significance level.

This feedback might be explained by weakened (enhanced) easterlies in the eastern Pacific

---

<sup>2</sup>The qualitative results presented in the following are unaltered if a strip over the whole equatorial Atlantic is chosen instead of Atl3.

basin in response to a warm (cold) equatorial Atlantic. This could produce upwelling (downwelling) Kelvin waves in the central basin, responsible for a cooling (warming) of SST in the Niño3 region. However, this is speculation at this point but should be subject of further research.

As in the previous section, to estimate the importance of the feedback from the Atlantic on the Pacific, an alternative model is fit to observations that is similar to (3) except that no feedback is included. The fitted parameters are  $\gamma_P = 0.040 \pm 0.011$ ,  $\omega_P = 0.133 \pm 0.022$ ,  $\gamma_A = 0.073 \pm 0.020$  and  $c_{AP} = 0.037 \pm 0.040$ . As done for the Indian Ocean, the models are integrated using this parameters and an additional stochastic forcing. The variance and correlation of the noise forcing are chosen to meet  $\sigma_{\xi_{hP}} = 0.6 \cdot \sigma_{\xi_{hI}}$  and the correlation between  $\xi_P$  and  $\xi_h$  is 0.2. For the model with feedback  $\sigma_{\xi_{TA}} = 1.65 \cdot \sigma_{\xi_{TP}}$  while for the model without feedback  $\sigma_{\xi_{TI}} = 1.6 \cdot \sigma_{\xi_{TP}}$ .

The cross-correlation of the model with feedback is in general agreement with observations (Fig. 14). The model correlation indeed fits better to the observational cross-correlation calculated from the maximum available time series than to the shorter period used for the parameter fits. This might seem counterintuitive at first glance but is reasonable if the model is assumed to be correct and the underlying physics are assumed to be stationary. In both, model and observational SSTA data, maximum correlation is found with positive (negative) Atl3 SSTA leading negative (positive) Niño3 SSTA. This lead-correlation, which was already mentioned by Keenlyside and Latif (2007), is not reproduced by the model without a feedback from the Atlantic on ENSO and raises hope for an improvement of ENSO predictions by including equatorial Atlantic SSTA.

Figure 15 a) shows the power spectral density calculated with the parameters fitted for the Pacific-Atlantic coupled model, compared to the observed Niño3 SST spectrum, from 1870-2003 HadISST data. As for the Pacific-Indian Ocean model and the Pacific only model (not shown), the model spectrum fits well with observations except of a tendency to reveal a more pronounced peak and therefore a more regular behavior. Figure 15 b) shows the influence of the Atlantic Ocean feedback on ENSO. Compared to the influence of the Indian Ocean feedback, the influence of the Atlantic Ocean feedback on ENSO variability is small. If the feedback is switched off (which means here that  $ch_{PA}$  and  $c_{PA}$  are set to zero) the total variance is reduced by 6% while the peak frequency (like the eigenfrequency) hardly changes at all.

Figure 16 compares Niño3 SSTA prediction skill of the coupled model to the prediction skill of the simplest recharge oscillator model without a feedback from ENSO. Even though the difference is small, some improvement is found for both cross validated time periods at all lead times.

## 6. Summary and Discussion

The questions addressed here were whether a mechanism analogous to that of ENSO also exists in the Atlantic or Indian Ocean and whether possible feedbacks of the tropical Indian and Atlantic Oceans on ENSO exist. We compared the observed Bjerknes and delayed negative feedbacks of the three tropical oceans and used an inverse modeling approach, with simple conceptual models fit to observations as hypotheses for the coupled dynamics. The results are analyzed in terms of the capability of the model to reproduce observed behavior and the implications of the determined parameters for the dynamics of the system. The model parameters obtained can obviously only provide information about the presence of particular coupled dynamics proposed by the model and we also need to note that the limited observational data may prevent us from using more complex models even though they may seem desirable. However,

where the model is capable of reproducing the observed variability (statistics), one can have some confidence, that the most important mechanisms are captured.

The observed Atlantic Ocean variability is well described by a simple model similar to the recharge oscillator model proposed by Jin (1997). A delayed negative feedback on SSTA via a recharge/discharge of equatorial heat content is found to be active in the equatorial Atlantic. The feedbacks are found to be strong enough to support a damped oscillatory mixed ocean dynamics-SST mode from boreal spring to late boreal fall, while two purely damped eigenmodes are found during the remaining part of the year. Figure 17 summarizes the monthly eigenvalues found for the different basins using the recharge oscillator model. It shows that the Atlantic model has quite similar dynamics as the Pacific model, except for a stronger damping, indicating a weaker Bjerknes feedback. Also the mean frequency found for the Atlantic is quite similar in the Pacific. The spectrum of the recharge oscillator for the Atlantic reveals somewhat enhanced variance on time scales around 4 years, compared to a red noise process. The results are in agreement with Zebiak (1993), who found a damped oscillation with a period of about 4 years in a Zebiak and Cane (1987) -type model for the Atlantic. However it is somewhat in disagreement with the results of Latif and Grötzner (2000) who find a quasi-biennial mode in the equatorial Atlantic from observational data.

It was also shown that the recharge oscillator model, using equatorial averaged thermocline depth anomalies, has predictive skill above persistence for Atl3 SSTA. In contrast a simple red noise model for Atl3 SSTA with an additional forcing from ENSO has hardly any forecast skill above persistence. However, it has to be noted that remote forcing from the Pacific or elsewhere may interact with the local dynamics in a way that can not be represented in our simple linear model.

Results for equatorial Indian Ocean variability were quite different to those of the Pacific and Atlantic Oceans. While there are indications for a positive feedback in the eastern Indian Ocean during July to September, associated with coastal upwelling off Sumatra (see also Chang et al. (2006b) and references herein), this seems to be quite different from the basin-wide Bjerknes feedback found in the Pacific and Atlantic Ocean. Probably the main reason for this is that heat content anomalies are not dominant in forcing SST variability. Moreover, a recharge-discharge mechanism of equatorial heat content, connected with the equatorial east-west SST gradient, which is found in the Pacific and Atlantic Oceans can not be identified in the Indian Ocean. The analysis rather suggest a mostly uncoupled damped system. This result is independent of the exact choice of the SST index and is found using the (-)DMI as well as an eastern Indian Ocean Box only.

The damping of the DMI mode is on average stronger than that of the other tropical oceans. However, it has a minimum in boreal summer, suggesting that a possible positive feedback acts predominantly during this time of the year. Forecast experiments with the recharge oscillator model fitted to the Indian Ocean show no significant skill for the DMI.

The somewhat negative result for the Indian Ocean may raise some questions on how this should be interpreted. There are basically two lines of thinking: First, as we interpreted the results above, the large scale statistics of the SST and heat content is mostly consistent with nearly uncoupled damped variability. A second, alternative, interpretation may be that the ocean-atmosphere interaction are more complex and maybe non-linear, which can simply not be captured by the simple model used in this study. The differences between the Indian Ocean and the other two is already reflected in the much warmer mean state and in the deep thermocline in the east of the basin. It may suggest that a different type of model (which is not included in the possible parameter space of eqs. 1) may find a stronger ocean-atmosphere coupled mode.

However, this interpretation is challenged by the relative good agreement of the model (used in this study) with the observed statistics of the SST. Any alternative model need to find a better fit to observations, with the same limited number of parameters.

Concerning the feedback from the Indian Ocean on ENSO, this study suggests that a warm(cold) Indian Ocean causes a cooling(warming) in the eastern Pacific and a shallowing of the equatorial averaged thermocline in the Pacific, due to changes in the Walker circulation. If this feedback is switched off in the simple model proposed here, the ENSO period shifts from about 4 to about 5 years and the total variance of Niño3 SSTA is increased by about 40%. The feedback is in agreement with the results of Wu and Kirtman (2004) and Kug and Kang (2006). The resulting influence of the tropical Indian Ocean on ENSO periodicity is also in agreement with Wu and Kirtman (2004) and with Dommenges et al. (2006). However, while Wu and Kirtman (2004) find an amplifying influence of the Indian Ocean on ENSO variability in their GCM experiments, we find that the Indian Ocean damps ENSO variability, which is in agreement with Dommenges et al. (2006). The different findings of Wu and Kirtman (2004) concerning the Indian Ocean influence on ENSO variance can be explained in the conceptual model, if parameters corresponding to the shorter ENSO frequency and to weaker coupling of the Indian Ocean SST on ENSO in their GCM are used.

Even though it was shown that the Indian Ocean has a considerable influence on the ENSO cycle, the forecast skill for Niño3 SSTA of the simple models used here could hardly be improved by explicitly including a feedback from the equatorial Indian Ocean. This can be explained by the fact that, at least in this model, Indian Ocean SSTA predictability is primarily limited to the SSTA caused by ENSO. The feedback of ENSO-induced Indian Ocean SSTA back on ENSO, however, is implicitly included if the uncoupled recharge oscillator is fitted to Pacific data only.

The coupling of equatorial Atlantic SSTA on ENSO is found to be much weaker than the coupling of the Indian Ocean on ENSO. However, a feedback from the equatorial Atlantic on ENSO is found with a warm(cold) Atlantic causing a cooling(warming) in the Niño3 region and a shallowing(deepening) of the equatorial averaged thermocline in the Pacific, which is similar to the feedback of the Indian Ocean on ENSO. The result are also in support of the finding of Wang (2006). The ENSO oscillation period or variance is, however, hardly influenced by this feedback. This is in disagreement with the CGCM results of Dommenges et al. (2006), who found a considerable frequency shift to longer periods if the tropical Atlantic is decoupled, which may be explained by the strong response of Atlantic Ocean SSTA on ENSO quite similar to the Indian Ocean, which is an artifact of the GCM used by Dommenges et al. (2006).

Even though the feedback from the Atlantic Ocean on ENSO is found to be weaker than that of the Indian Ocean, the forecast skill for Niño3 SSTA could be improved, if a feedback from the Atlantic on ENSO is included. This improvement is stronger than that from including the Indian Ocean, because the Atlantic SSTA itself is more independent from ENSO.

The two-way interactions we found between the tropical Pacific and the other two tropical oceans, raise the questions, if the other two oceans are also interacting with each other or what is the combined effect of both oceans onto the tropical Pacific. Additional analysis with the conceptual models indicate that the prediction skill, if both Indian and Atlantic ocean are coupled to the tropical Pacific is approximately the same as for the model with feedback from the Atlantic only (not shown). If, however, an additional coupling between Indian and Atlantic Ocean is included (now all oceans interact in both ways), significant coupling of Indian Ocean SSTA on Atl3 SSTA is found, with warm (cold) Atl3 SSTA causing warming (cooling) in the Indian Ocean. The forecast skill for Niño3 SSTA in this model is slightly improved, approxi-

mately adding together the improvements gained by including each single Ocean (not shown). However, these results include many fitted parameters and need further detailed studies.

The study presented above relies on the quality of the data used, especially for subsurface data. To test the robustness of our findings, the complete analysis was therefore redone using SODA (Carton et al., 2000) subsurface and SST data. We find that the qualitative results change little. The major differences are: The forecast skill of the recharge oscillator for the Atlantic is somewhat worse if SODA data is used. This suggests that the MPIOM produces more reliable subsurface data here, since it is unlikely that worse subsurface data produces better forecast skill for observed SSTA. The damping found for the DMI becomes negative (i.e. positive growth rate) during the summer months, which supports the hypothesis that a positive feedback exists during this time of the year. However, since a recharge/discharge mechanism is still not found in the Indian Ocean, the eigenvalues are strictly real for the whole year.

#### *Acknowledgments.*

We like to thank the anonymous reviewers for helpful comments, which improved the presentation of this analysis significantly. The OGCM simulation was kindly provided by Peter Korn and performed at the Deutsches Klimarechenzentrum. This work was supported by the European Union Dynamite (GOCE 00393) and AMMA (GOCE 004089) project and by the Deutsche Forschungs Gesellschaft project (DO1038/2-1).

## References

- Annamalai, H., S. Xie, J. McCreary, and R. Murtugudde, 1995: Impact of Indian Ocean Sea Surface Temperature on Developing El Niño. *J. Climate*, **18**, 302–319.
- Baquero-Bernal, A., M. Latif, and S. Legutke, 2002: On dipolelike variability of sea surface temperature in the tropical Indian Ocean. *J. Climate*, **15** (11), 1358–1368.
- Battisti, D. S. and A. C. Hirst, 1989: Interannual variability in a tropical atmosphere-ocean model: influence of the basic state, ocean geometry and nonlinearity. *J. Atmos. Sci.*, **46** (12), 1687–1712.
- Behera, S. K., J. Luo, S. Masson, S. Rao, and H. Sakuma, 2006: A cpcm study on the interaction between iod and enso. *J. Climate*, **19**, 1688–1705.
- Behera, S. K., S. A. Raa, H. N. Saji, and T. Yamagata, 2003: Comments on “A cautionary note on the interpretation of EOFs”. *J. Climate*, **16**, 1087–1093.
- Burgers, G., F.-F. Jin, and G. J. van Oldenborgh, 2005: The simplest ENSO recharge oscillator. *Geophys. Res. Lett.*, **32**, L13 706, doi:10.1029/2005GL022951.
- Carton, J. A., G. Chepurin, X. Cao, and B. Giese, 2000: A simple ocean data assimilation analysis of the global upper ocean 1950-1995, part 1: methodology. *J. Phys. Oceanogr.*, **30**, 294–309.
- Chang, P., Y. Fang, R. Saravanan, L. Ji, and H. Seidel, 2006a: The cause of the fragile relationship between the pacific el niño and the atlantic niño. *Nature*, **443**, doi:doi:10.1038/nature05053.
- Chang, P., T. Yamagata, P. Schopf, S. K. Behera, J. Carton, W. S. Keesler, G. Meyers, T. Qu, F. Schott, S. Shetye, and S.-P. Xie, 2006b: Climate fluctuations of tropical coupled systems - The role of ocean dynamics. *J. Climate*, **19** (20), 5122–5174.
- Davis, R. E., 1976: Predictability of sea surface temperature and sea level pressure anomalies over the north Pacific ocean. *J. Phys. Oceanogr.*, **6**, 249–266.
- Dominiak, S. and P. Terray, 2005: Improvement of enso prediction using a linear regression model with a southern indian ocean sea surface temperature predictor. *Geophys. Res. Lett.*, **32**, L18 702, doi:10.1029/2005GL023153.
- Dommenget, D. and M. Latif, 2002: A cautionary note on the interpretation of EOFs. *J. Climate*, **15**, 216–225.
- , 2003: Reply. *J. Climate*, **16**, 1094–1097.
- Dommenget, D., V. Semenov, and M. Latif, 2006: Impacts of the tropical Indian and Atlantic Oceans on ENSO. *Geophys. Res. Lett.*, **33**, L11 701, doi:10.1029/2006GL025871.
- Enfield, D. B. and D. A. Mayer, 1997: Tropical Atlantic sea surface temperature variability and its relation to El Niño-Southern Oscillation. *J. Geophys. Res.*, **102**, 929–945.

- Fischer, A., P. Terray, P. Delecluse, S. Gualdi, and E. Guilyardi, 2005: Two independent triggers for the indian ocean dipole/zonal mode in a coupled gcm. *J. Climate*, **18**, 3428–3449.
- Frankignoul, C. and K. Hasselmann, 1977: Stochastic climate models. part ii. application to SST anomalies and thermocline variability. *Tellus*, **29**, 289–305.
- Gualdi, S., E. Guilyardi, A. Navarra, S. Masina, and P. Deleclus, 2003: The interannual variability in the tropical indian ocean as simulated by a cgcm. *Climate Dyn.*, **20**, 567–582.
- Huang, B., 2004: Remotely forced variability in the tropical Atlantic ocean. *Climate Dyn.*, **23**, 133–152.
- Jin, F.-F., 1997: An equatorial recharge paradigm for ENSO, part 1:conceptual model. *J. Atmos. Sci.*, **54**, 811–829.
- Kalnay, E. et al., 1996: The NCEP/NCAR 40-year reanalysis project. *Bull. Am. Meteorol. Soc.*, **77**, 437–471.
- Keenlyside, N. S. and M. Latif, 2007: Understanding equatorial Atlantic interannual variability. *J. Climate*, **20**, 131–142.
- Kug, J.-S. and I.-S. Kang, 2006: Interactive feedback between ENSO and the Indian Ocean. *J. Climate*, **19** (9), 1784–1801.
- Latif, M. and A. Grötzner, 2000: The equatorial Atlantic oscillation and its response to ENSO. *Climate Dyn.*, **16**, 213–218.
- Levitus, S., R. Burgett, and T. P. Boyer, 1994: *World Ocean Atlas, 1994*, Salinity, NOAA Atlas NESDIS 3, Vol. 3. Natl. Oceanogr. Data Cent., Silver Springs, Md., 111 pp.
- Marsland, S., H. Haak, J. Jungclaus, and M. Latif, 2003: The Max-Planck-Institute global ocean/sea ice model with orthogonal curvilinear coordinates. *Ocean Model.*, 91–127.
- Meinen, C. S. and M. J. McPhaden, 2000: Observations of Warm Water Volume Changes in the Equatorial Pacific and Their Relationship to El Niño and La Niña. *J. Climate*, **13**, 3551–3559.
- Meyers, G., P. McIntosh, L. Pigot, and M. Pook, 2007: The years of el nio, la nia, and interactions with the tropical indian ocean. *J. Climate*, **20**, 28722880.
- Okumura, Y. and S.-P. Xie, 2006: Some overlooked features of tropical Atlantic climate leading to a new Niño-like phenomenon. *J. Climate*, **19**, 5859–5874.
- Rayner, N. A., D. E. Parker, E. B. Horton, C. K. Folland, L. V. Alexander, D. P. Rowell, E. C. Kent, and A. Kaplan, 2003: Global analyses of sea surface temperature, sea ice, and night marine air temperature since the late nineteenth century. *J. Geophys. Res.*, **108** (D14), 4407, doi:10.1029/2002JD002670.
- Ruiz-Barradas, A., J. A. Carton, and S. Nigam, 2000: Structure of interannual-to-decadal climate variability in the tropical Atlantic sector. *J. Climate*, **13**, 3285–3297.
- Saji, N., B. Goswami, P. Vinayachandran, and T. Yamagata, 1999: A dipole mode in the tropical Indian Ocean. *Nature*, **401** (6751), 360–363.

- Saravanan, R. and P. Chang, 2000: Interaction between tropical Atlantic variability and El Niño-Southern Oscillation. *J. Climate*, **13**, 2177–2194.
- Song, Q., G. Vecchi, and A. Rosati, 2007: Indian ocean variability in the gfdl cm2 coupled climate model. *J. Climate*, **20**, 2895–2916.
- Suarez, M. J. and P. S. Schopf, 1988: A delayed action oscillator for ENSO. *J. Atmos. Sci.*, **45** (21), 3283–3287.
- Venzke, S., M. Latif, and A. Villwock, 2000: The coupled GCM Echo-2. Part II: Indian Ocean response to ENSO. *J. Climate*, **13** (8), 1371–1383.
- Wang, C., 2006: An overlooked feature of tropical climate: Inter-pacific-atlantic variability. *Geophys. Res. Lett.*, **33**, L12 702.
- Webster, P., A. Moore, J. Loschnigg, and R. Leben, 1999: Coupled ocean-atmosphere dynamics in the Indian Ocean during 1997-98. *Nature*, **401** (6751), 356–360.
- Wu, R. and B. P. Kirtman, 2004: Understanding the impacts of the Indian Ocean on ENSO variability in a coupled GCM. *J. Climate*, **17** (20), 4019–4031.
- Xie, S.-P., H. Annamalai, F. A. Schott, and J. P. McCreary, 2002: Structure and mechanisms of south Indian Ocean climate variability. *J. Climate*, **15**, 864–878.
- Yeh, S.-W., R. Wu, and B. Kirtman, 2007: Impact of the indian ocean on enso variability in a hybrid coupled model. *Quart. J. Roy. Meteor. Soc.*, **133**, 445–45.
- Yu, J., 2005: Enhancement of enso's persistence barrier by biennial variability in a coupled atmosphere-ocean general circulation model. *Geophys. Res. Lett.*, **32**, L13 707.
- Yu, J.-Y., C. R. Mechoso, J. C. McWilliams, and A. Arakawa, 2002: Impacts of the Indian Ocean on the ENSO cycle. *Geophys. Res. Lett.*, **29** (8), 1204, doi: doi:10.1029/2001GL014098.
- Zebiak, S. E., 1993: Air-sea interaction in the equatorial Atlantic region. *J. Climate*, **6**, 1567–1586.
- Zebiak, S. E. and M. A. Cane, 1987: A model El Niño-Southern Oscillation. *Mon. Wea. Rev.*, **115**, 2262–2278.

# List of Figures

1	<p>The three elements of the Bjerknes feedback in the different tropical oceans: <b>(a)</b> Regression of SSTA indices on surface zonal wind stress anomalies of the same ocean basin (<math>10^{-2} Pa K^{-1}</math>). The SSTA indices (boxes) are the Niño3 , Atl3, and (-)DMI. <b>(b)</b> Regression of surface zonal wind stress anomaly indices on 20°C-isotherm depth anomalies in the same ocean basin (<math>m(10^{-2} Pa)^{-1}</math>). The indices (boxes) are the Niño4, WAtl and IEq. <b>(c)</b> Regression of 20°C-isotherm depth anomalies on SSTA (<math>K(10^{-2} m)^{-1}</math>). The period considered is 1950-2001. The boundaries between individual ocean basins in (a) and (b) are indicated by thick black lines. Explained variance are overlaid with a 0.1 contour interval starting 0.05 and values greater than 0.06, 0.07, and 0.07 are significant at the 95% level in (a), (b), and (c), respectively. . . . .</p>	21
2	<p><b>(a)</b> Cross-correlation between SSTA indices and zonal wind stress anomalies indices of the three tropical oceans. <b>(b)</b> Cross-correlation between 20°C-isotherm depth anomalies indices and SSTA indices of the three tropical oceans. Correlations above 0.25 and 0.27 are significant at the 95% level in (a) and (b), respectively. . . . .</p>	22
3	<p>Seasonally resolved cross correlation <b>(a)</b> between observed Niño3 SSTA and equatorial Pacific warm water volume anomalies (WWV); <b>(b)</b> Atl3 SSTA and equatorial Atlantic WWV; and <b>(c)</b> (-)DMI SSTA and equatorial Indian Ocean WWV. WWV is defined as the 5°S-5°N average 20-degree isotherm depth and is taken from an NCEP-forced OGCM run. The time period is 1950-2001. Correlations of 0.3 are significant on a 95% level. . . . .</p>	23
4	<p><b>a)</b> Seasonal cycle of the eigenvalues of the recharge oscillator with the parameters fitted to Atlantic observational SST data and thermocline depth data from an NCEP forced GCM run, for the time period 1950-2001. Error bars denote 95% confidence levels and are estimated using a monte-carlo method and assuming independent, normally distributed errors for the parameters. <b>b)</b> The same for the Pacific Ocean . . . . .</p>	24
5	<p>Seasonally resolved cross correlation between equatorial Atlantic thermocline depth anomalies and Atl3 SSTA, as in fig. 3b, but for the recharge oscillator model with stochastic excitation. . . . .</p>	25
6	<p><b>a)</b> Eastern Atlantic SST spectrum of the recharge oscillator model with stochastic excitation (red), compared to the observed Atl3 SST spectrum from 1870 to 2003(black). The thin red lines show the 95% confidence interval. <b>b)</b> The model spectrum compared to an AR1 process fitted to observational data in a linear scale. The thin vertical black lines denote a frequency of four years in both plots. . . . .</p>	26
7	<p><b>a)</b> Forecast skill of the recharge oscillator model for the Atlantic. Shown is the anomaly correlation between predicted and observed Atl3 SSTA, compared to the observed autocorrelation (Persistence). The coloured lines show cross validated forecast skills. The time intervals given in the legend refer to the period used for the forecast skill evaluation, while in each case the other interval was used to fit the parameters. For the black line the whole time period was used for the parameter fit and for the evaluation of forecast skill. <b>b)</b> The same for an AR1 model with an additional coupling to observed Niño3 SSTA. . . . .</p>	27

8	As figure 4, but for Indian Ocean data . . . . .	28
9	As figure 5, but for Indian Ocean (-)DMI and thermocline depth. . . . .	29
10	<b>a)</b> As figure 7 but for DMI predictions with the Indian Ocean recharge oscillator model. <b>b)</b> the same for an AR1 model with an additional coupling to observed Niño3 SSTA <b>c)</b> as b but for equatorial Indian Ocean SSTA averaged over the whole basin ( $5^{\circ}S - 5^{\circ}N, 40^{\circ}E - 110^{\circ}E$ ) . . . . .	30
11	Left: Cross correlation between Niño3 SSTA and equatorial Indian Ocean SSTA for the Pacific-Indian Ocean coupled model (red) compared to observational data from the period 1870-2003(blue) and 1950-2003(green). Correlations above 0.33(0.17) are significant at the 95% level, assuming 34(134) degrees of freedom. Right: The same for the model without a feedback from the Indian Ocean on ENSO (The parameters for the two models are fitted separately). . . . .	31
12	<b>a)</b> Niño3 SST spectrum of the Pacific-Indian Ocean coupled model(red) compared to HadISST observational data from 1870 to 2003 (black). The thin red lines show the 95% confidence interval. <b>b)</b> Model spectrum (red) compared to the spectrum of the same model, but with the feedback parameters $c_{PI}$ and $ch_{PI}$ set to zero (black). The thin vertical lines denote the eigenfrequencies, which are $48.5 \text{ month}^{-1}$ for the fully coupled model and $60.5 \text{ month}^{-1}$ if the feedback is switched of. (plotted is frequency times power spectral density) . . . . .	32
13	as Figure 7 but for $T_p$ of the Pacific-Indian Ocean coupled model (solid lines), compared to the simplest recharge oscillator ENSO model, without explicit consideration of the Indian Ocean (dashed lines). . . . .	33
14	Left: As figure 11, but between Niño3 SSTA and Atl3 SSTA for the Pacific-Atlantic Ocean coupled model (red) compared to observational HadISST data from the period 1870-2003(blue) and 1950-2003(green). Right: The same for the model without a feedback from the Atlantic on ENSO (The parameters for the two models are fitted separately) . . . . .	34
15	As figure 12 but for the Pacific-Atlantic coupled model. The thin vertical lines denote the eigenfrequencies, which are $49.5 \text{ month}^{-1}$ for the fully coupled model and $51 \text{ month}^{-1}$ if the feedback is switched of, (plotted is frequency times power spectral density). . . . .	35
16	As figure 13 but for the Pacific-Atlantic coupled model. . . . .	36
17	Monthly eigenvalues of the recharge oscillator model for the Pacific (blue), the Atlantic (green) and the Indian Ocean (red). In case of real eigenvalues, the bigger and smaller values are marked by a cross and a circle, respectively. As discussed in the text, in the Indian Ocean, the strongest damped eigenvalues belong to an approximate SST-mode. . . . .	37

## List of Figures

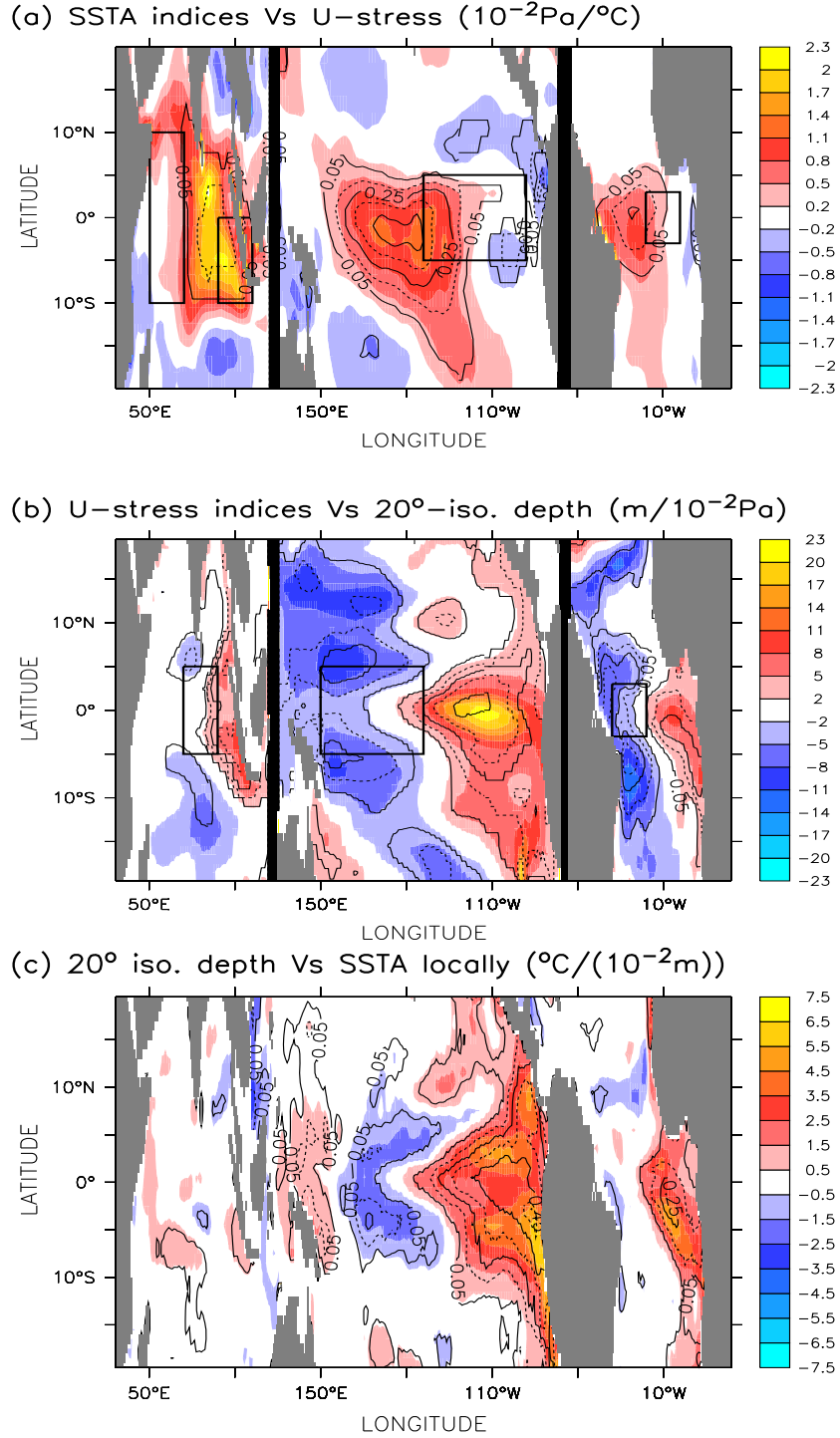
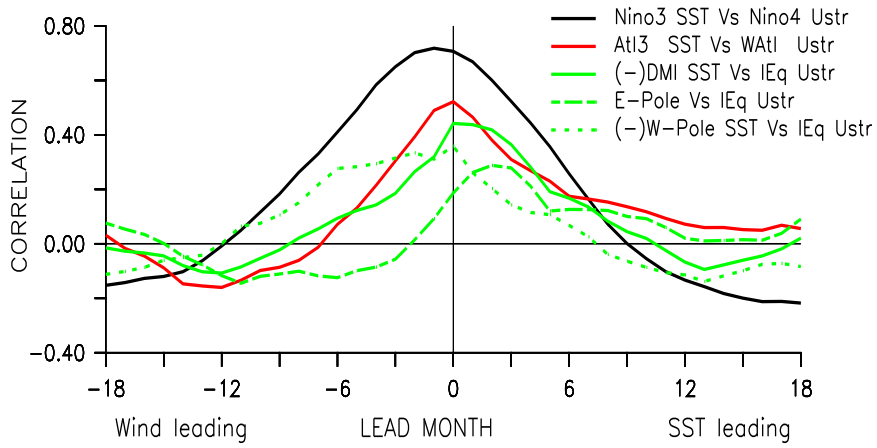


FIG. 1. The three elements of the Bjerknes feedback in the different tropical oceans: **(a)** Regression of SSTA indices on surface zonal wind stress anomalies of the same ocean basin ( $10^{-2}PaK^{-1}$ ). The SSTA indices (boxes) are the Niño3 , Atl3, and (-)DMI. **(b)** Regression of surface zonal wind stress anomaly indices on  $20^\circ C$ -isotherm depth anomalies in the same ocean basin ( $m(10^{-2}Pa)^{-1}$ ). The indices (boxes) are the Niño4, WAtl and IEq. **(c)** Regression of  $20^\circ C$ -isotherm depth anomalies on SSTA ( $K(10^{-2}m)^{-1}$ ). The period considered is 1950-2001. The boundaries between individual ocean basins in (a) and (b) are indicated by thick black lines. Explained variance are overlaid with a 0.1 contour interval starting 0.05 and values greater than 0.06, 0.07, and 0.07 are significant at the 95% level in (a), (b), and (c), respectively.

(a) SST Vs U-Stress



(b) 20° Iso. depth Vs SST

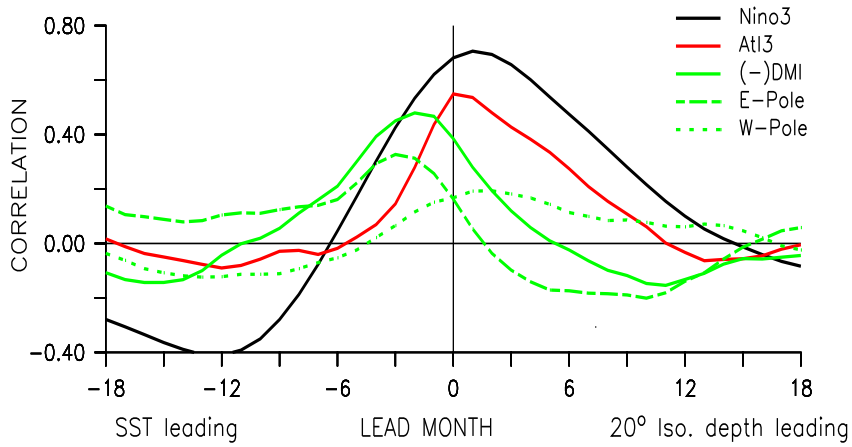


FIG. 2. **(a)** Cross-correlation between SSTA indices and zonal wind stress anomalies indices of the three tropical oceans. **(b)** Cross-correlation between 20°C-isotherm depth anomalies indices and SSTA indices of the three tropical oceans. Correlations above 0.25 and 0.27 are significant at the 95% level in (a) and (b), respectively.

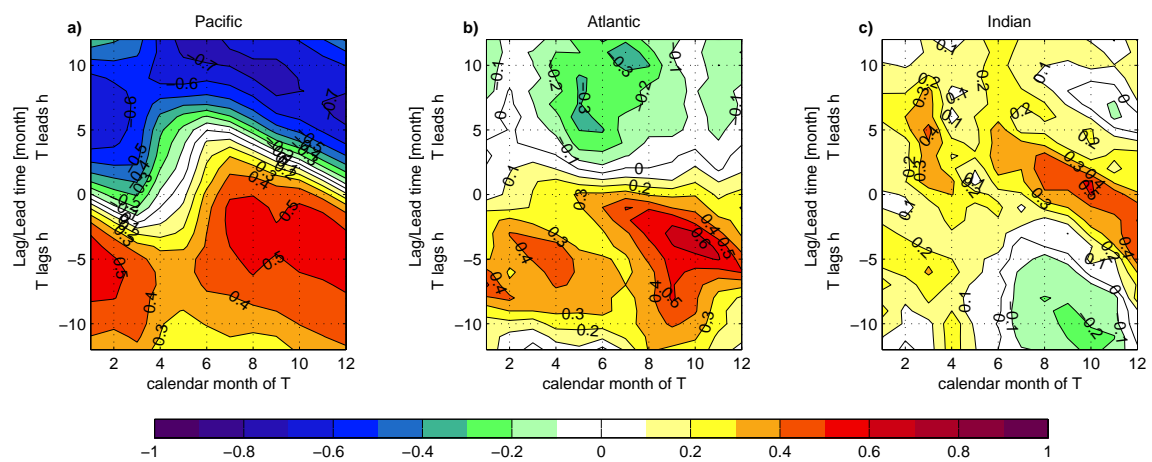


FIG. 3. Seasonally resolved cross correlation **(a)** between observed Niño3 SSTA and equatorial Pacific warm water volume anomalies (WWV); **(b)** Atl3 SSTA and equatorial Atlantic WWV; and **(c)** (-)DMI SSTA and equatorial Indian Ocean WWV. WWV is defined as the  $5^{\circ}\text{S}$ - $5^{\circ}\text{N}$  average 20-degree isotherm depth and is taken from an NCEP-forced OGCM run. The time period is 1950-2001. Correlations of 0.3 are significant on a 95% level.

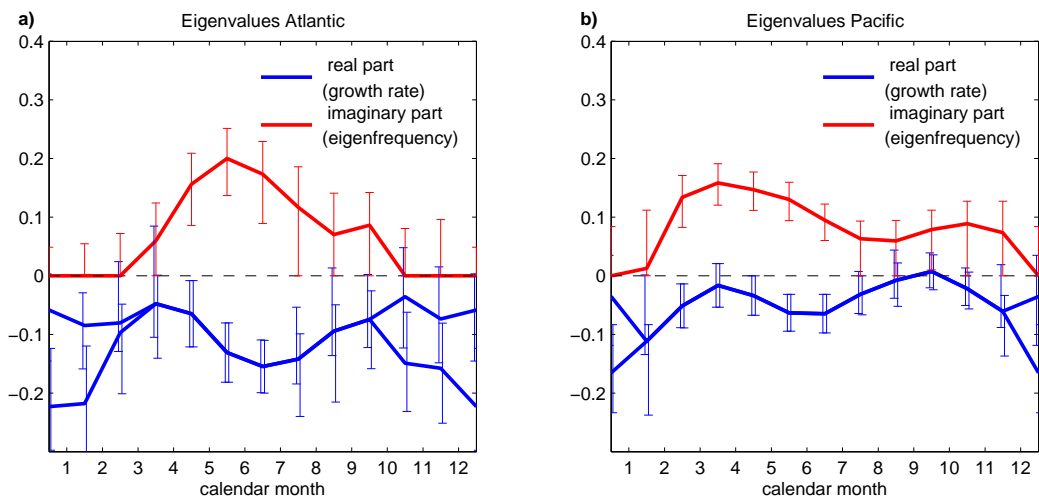


FIG. 4. **a)** Seasonal cycle of the eigenvalues of the recharge oscillator with the parameters fitted to Atlantic observational SST data and thermocline depth data from an NCEP forced GCM run, for the time period 1950-2001. Error bars denote 95% confidence levels and are estimated using a monte-carlo method and assuming independent, normally distributed errors for the parameters. **b)** The same for the Pacific Ocean

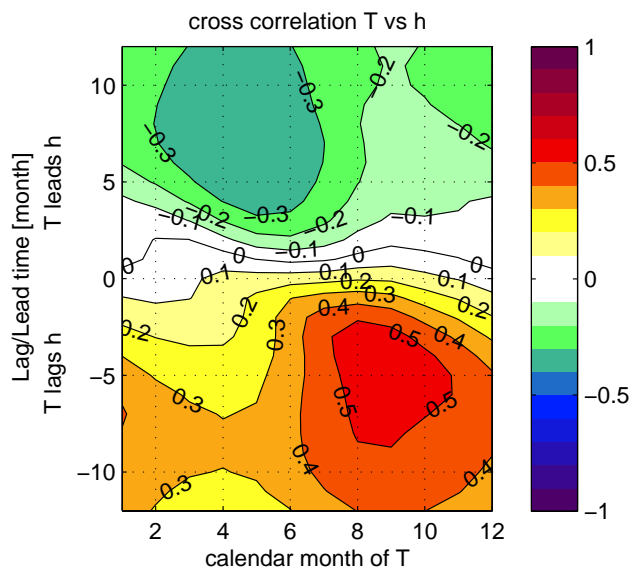


FIG. 5. Seasonally resolved cross correlation between equatorial Atlantic thermocline depth anomalies and Atl3 SSTA, as in fig. 3b, but for the recharge oscillator model with stochastic excitation.

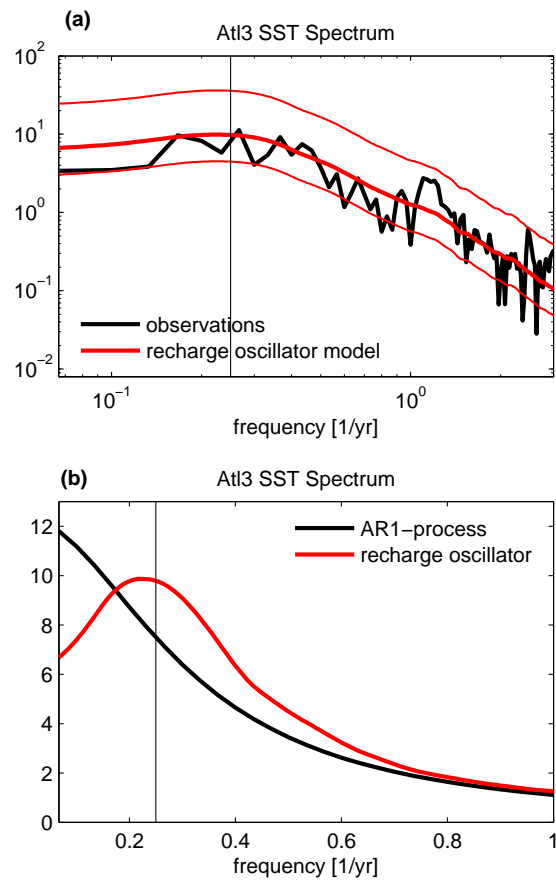


FIG. 6. **a)** Eastern Atlantic SST spectrum of the recharge oscillator model with stochastic excitation (red), compared to the observed At13 SST spectrum from 1870 to 2003 (black). The thin red lines show the 95% confidence interval. **b)** The model spectrum compared to an AR1 process fitted to observational data in a linear scale. The thin vertical black lines denote a frequency of four years in both plots.

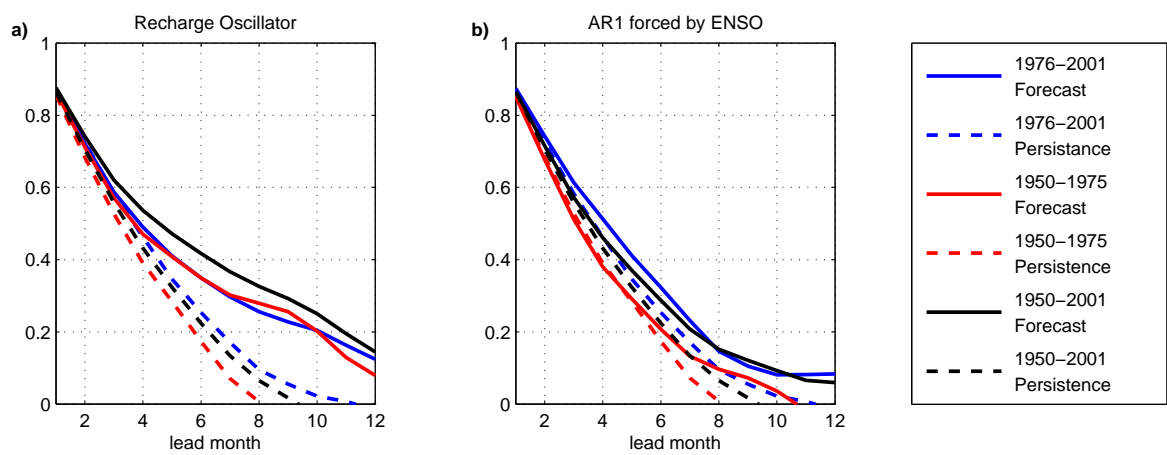


FIG. 7. **a)** Forecast skill of the recharge oscillator model for the Atlantic. Shown is the anomaly correlation between predicted and observed Atl3 SSTA, compared to the observed autocorrelation (Persistence). The coloured lines show cross validated forecast skills. The time intervals given in the legend refer to the period used for the forecast skill evaluation, while in each case the other interval was used to fit the parameters. For the black line the whole time period was used for the parameter fit and for the evaluation of forecast skill. **b)** The same for an AR1 model with an additional coupling to observed Niño3 SSTA.

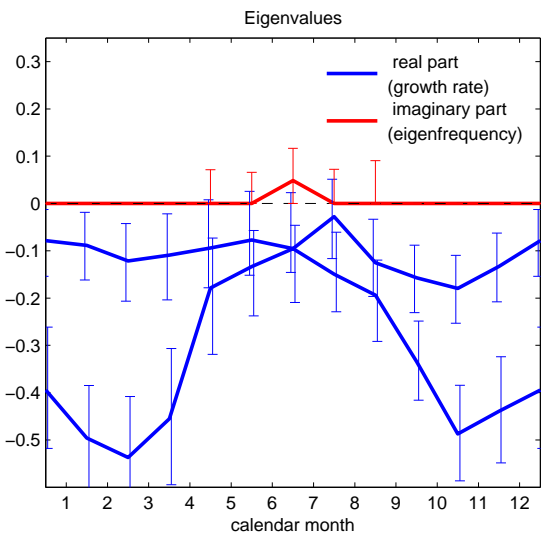


FIG. 8. As figure 4, but for Indian Ocean data

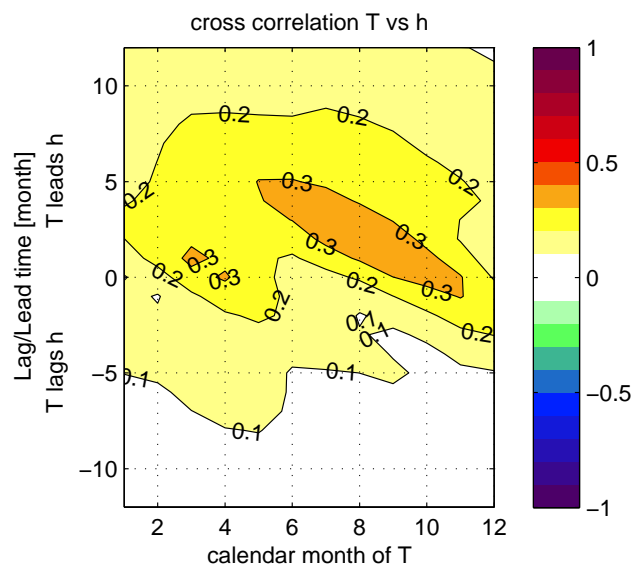


FIG. 9. As figure 5, but for Indian Ocean (-)DMI and thermocline depth.

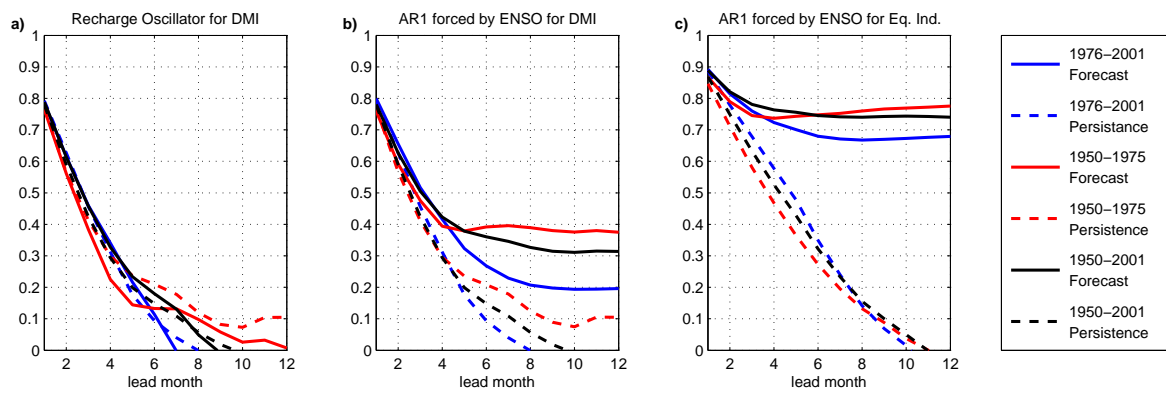


FIG. 10. **a)** As figure 7 but for DMI predictions with the Indian Ocean recharge oscillator model. **b)** the same for an AR1 model with an additional coupling to observed Niño3 SSTA **c)** as b but for equatorial Indian Ocean SSTA averaged over the whole basin ( $5^{\circ}S - 5^{\circ}N, 40^{\circ}E - 110^{\circ}E$ )

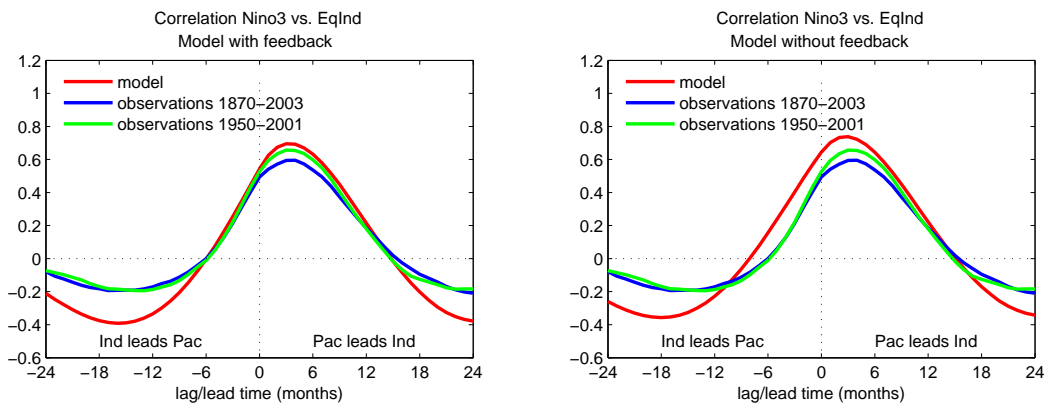


FIG. 11. Left: Cross correlation between Niño3 SSTA and equatorial Indian Ocean SSTA for the Pacific-Indian Ocean coupled model (red) compared to observational data from the period 1870-2003(blue) and 1950-2003(green). Correlations above 0.33(0.17) are significant at the 95% level, assuming 34(134) degrees of freedom. Right: The same for the model without a feedback from the Indian Ocean on ENSO (The parameters for the two models are fitted separately).

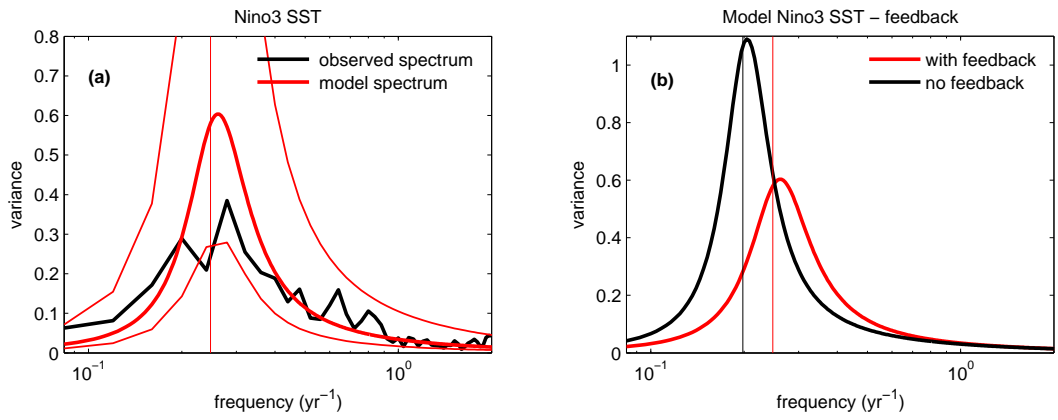


FIG. 12. **a)** Niño3 SST spectrum of the Pacific-Indian Ocean coupled model (red) compared to HadISST observational data from 1870 to 2003 (black). The thin red lines show the 95% confidence interval. **b)** Model spectrum (red) compared to the spectrum of the same model, but with the feedback parameters  $c_{PI}$  and  $ch_{PI}$  set to zero (black). The thin vertical lines denote the eigenfrequencies, which are  $48.5 \text{ month}^{-1}$  for the fully coupled model and  $60.5 \text{ month}^{-1}$  if the feedback is switched of. (plotted is frequency times power spectral density)

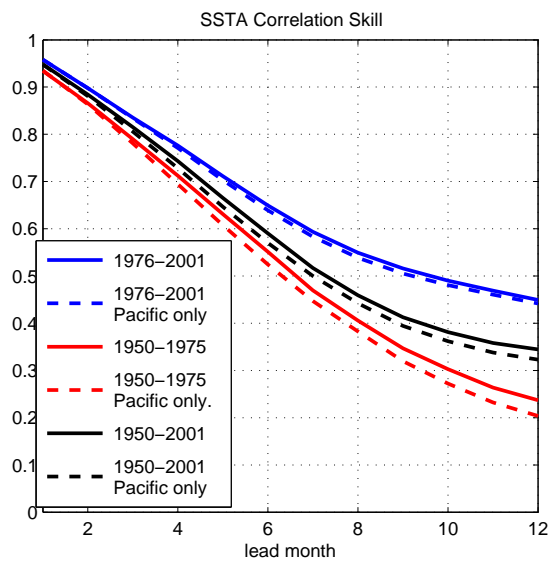


FIG. 13. as Figure 7 but for  $T_p$  of the Pacific-Indian Ocean coupled model (solid lines), compared to the simplest recharge oscillator ENSO model, without explicit consideration of the Indian Ocean (dashed lines).

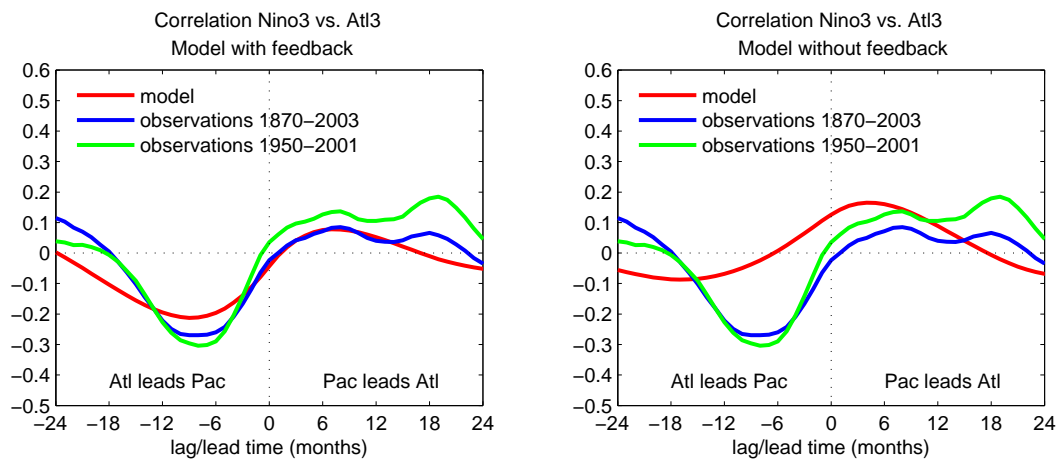


FIG. 14. Left: As figure 11, but between Niño3 SSTA and Atl3 SSTA for the Pacific-Atlantic Ocean coupled model (red) compared to observational HadISST data from the period 1870-2003(blue) and 1950-2003(green). Right: The same for the model without a feedback from the Atlantic on ENSO (The parameters for the two models are fitted separately)

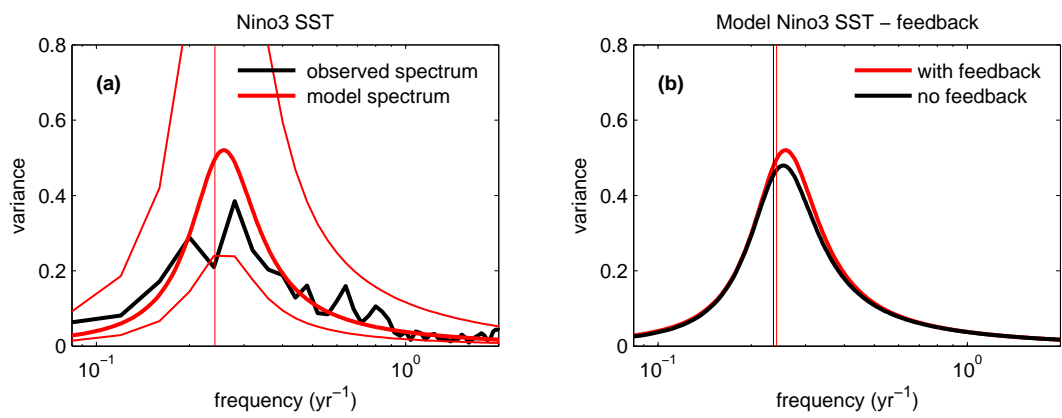


FIG. 15. As figure 12 but for the Pacific-Atlantic coupled model. The thin vertical lines denote the eigenfrequencies, which are  $49.5 \text{ month}^{-1}$  for the fully coupled model and  $51 \text{ month}^{-1}$  if the feedback is switched of, (plotted is frequency times power spectral density).

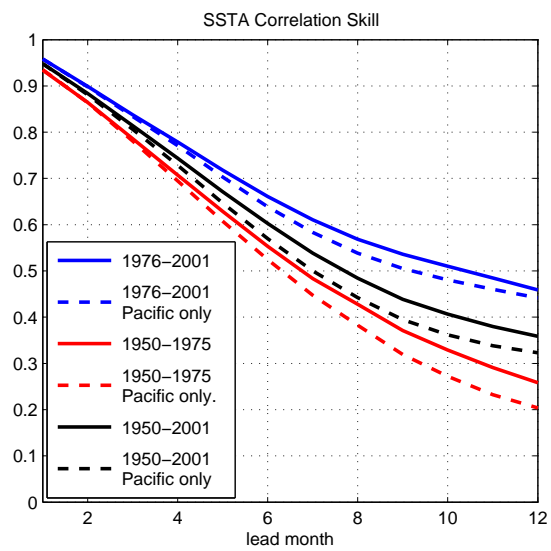


FIG. 16. As figure 13 but for the Pacific-Atlantic coupled model.

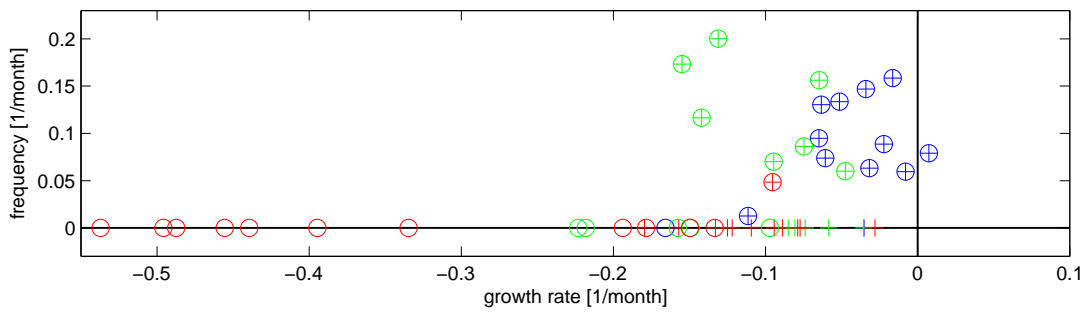


FIG. 17. Monthly eigenvalues of the recharge oscillator model for the Pacific (blue), the Atlantic (green) and the Indian Ocean (red). In case of real eigenvalues, the bigger and smaller values are marked by a cross and a circle, respectively. As discussed in the text, in the Indian Ocean, the strongest damped eigenvalues belong to an approximate SST-mode.

## List of Tables

1	Areas corresponding to the different indices used in the text. . . . .	39
---	--	----

TABLE 1. Areas corresponding to the different indices used in the text.

Niño3	150-90°W, 5°S-5°N
Niño4	150°E-150°W, 5°S-5°N
WWV - Pacific	130°E-80°W, 5°S-5°N
Atl3	20°W-0°E, 3°S-3°N
WAtl	40-20°W, 3°S-3°N
WWV - Atlantic	50°W-20°E, 5°S-5°N
(-)DMI	eastern pole (90-110°E, 10°S-0°N) - western pole (50-70°E, 10°S-10°N)
IEq	70-90°E, 5°S-5°N
EqInd	40°E-110°E, 5°S-5°N,
WWV - Indian	40-110°E, 5°S-5°N